ELSEVIER

Thermochimica Acta, 242 (1994) 161–172

thermochimica acta

Analysis of the direct sulfation of calcium carbonate

A.B. Fuertes *, G. Velasco, M.J. Fernandez, T. Alvarez

Instituto Nacional del Carbón, Apartado 73, 33080 Oviedo, Spain

(Received 6 November 1993; accepted 25 January 1994)

Abstract

The kinetics of the direct $CaCO_3$ particles is investigated. The experiments were carried out in a thermogravimetric analyzer under isothermal conditions between 740 and 890°C. A pure calcium carbonate sample with a mean size of 16 μm and a specific surface area of 0.6 $m^2 g^{-1}$ was used. The variation of reaction rate with temperature shows that the process is controlled by the chemical reaction. An activation energy of around 110–130 kJ mol^{-1} was measured. The dependence between chemical rate and temperature is given by $k_p = 740 \exp(-113000/RT)$ (mol m^{-2}) s atm. The process was modeled according to a shrinking unreacted core model. Whereas the CaO sulfation stops due to the blockage of external pores, the $CaCO_3$ sulfation does not exhibit abrupt changes in reactivity, probably due to the porosity of the production layer. The recarbonated samples show higher sulfation rates than uncalcinated $CaCO_3$ samples.

Keywords: Activation energy; Calcium carbonate; Model; Sulphation; TGA

1. Introduction

Sulfur dioxide emissions originating during fluidized-bed coal combustion may be reduced by the addition of calcium sorbents, i.e. limestone or dolomite. In combustors operating at atmospheric pressure (CO_2 partial pressure below 0.2 atm and temperatures above 800°C), the $CaCO_3$ calcination occurs prior to sulfation. Then, the sulfation reaction will occur between SO_2 and the porous CaO particles.

In pressurized combustors (CO_2 partial pressure around 1 atm and temperatures below 900°C), the calcium carbonate decomposition is thermodynamically unfa-

* Corresponding author.

SSDI 0040-6031(94)01731-U

vored. Under these circumstances, the sulfation reaction will take place according to

$$CaCO_3 + SO_2 + 0.5O_2 \rightarrow CaSO_4 + CO_2$$

Different studies of the $CaCO_3$–SO_2 reaction have been made by Snow et al. [1], Hajaligol et al. [2], Iise et al. [3, 4], Illerup et al. [5], Tullin et al. [6] and, recently, by our group [7, 8]. In all cases it was observed that the ultimate grade of sulfation via the $CaCO_3$–SO_2 reaction was higher than that reached in the case of the CaO–SO_2 reaction. This is attributed to the higher porosity of the product layer formed during direct sulfation of $CaCO_3$ than that corresponding to CaO sulfation, which enhances the diffusional transport of SO_2 in the former case. Some authors [2, 7, 9] have observed that the reaction is chemically controlled at low conversion degrees; activation energy around 80–100 kJ mol^{-1}. However, at higher conversion degrees, the process is controlled by diffusion through the product layer. Under these conditions, the values measured for activation energy are around 150 kJ mol^{-1}. The higher value of the activation energy under diffusional control suggests that mass transport through the product layer occurs by means of a solid-state ionic mechanism instead of by molecular diffusion (activation energy around 12 kJ mol^{-1}) or Knudsen diffusion (activation energy around 4 kJ mol^{-1}). Fuertes et al. [8] have postulated a mechanism for the direct sulfation under solid–ionic diffusional control, suggesting that CO_3^{2-} is the mobile species in ionic diffusion; the CO_3^{2-} diffuses through the $CaSO_4$ layer from the $CaCO_3$–$CaSO_4$ interface to the product layer surface and the SO_4^{2-} species counter-diffuses in the opposite sense.

The higher activation energy of the diffusional process than that corresponding to chemical reaction results from the fact that the reaction shifts towards chemical reaction control at higher temperatures and towards product layer diffusional control at lower temperatures [10]. This anomalous behavior makes it diffcult to distinguish between chemical control and diffusional control. In addition, the rate of the solid–ionic diffusion process will be influenced by impurities and crystalline defects [11]. In consequence, one should expect that impure materials, i.e. limestone or dolomite, exhibit clear differences in reactivity with respect to pure calcium carbonate. Thus, Hajaligol, et al. [2] found that pure calcite particles exhibited lower reactivity than impure limestone particles.

The main objective of this paper is to analyze the kinetics of the direct sulfation of pure calcium carbonate particles, over a range of temperatures typical of pressurized fluidized combustion. In addition, the direct sulfation reactions compared with the sulfation of calcined particles and the sulfation of recarbonated calcium oxide particles is examined.

2. Experimental

The experiments were performed with calcium carbonate (Analytical grade, Panreac) with less than 1.5% impurities. The particle size distribution, determined

using a Coulter Multisizer II, was found to range between 5 and 25 μm, with an averge size of 16 μm. The BET surface area, measured in nitrogen (−196°C), was 0.6 $m^2 g^{-1}$.

A thermogravimetric analyzer (Setaram Tag 24) was used in these experiments. The experimental procedure consisted of heating a sample at 40°C min^{-1}, in CO_2 or N_2 atmosphere, up to the desired temperature. When the isothermal condition was reached, a gas stream with a composition of 2600 ppm SO_2 and 3.4% O_2 was added. The gas composition was balanced with CO_2 (direct sulfation) or N_2 (CaO sulfation). In all experiments the sample weight was below 5 mg and the gas flow rate 100 ml min^{-1}. With these conditions, the reaction rate was found to be independent of external resistances.

3. Results and discussion

3.1. Influence of temperature on direct sulfation

Figure 1 shows the variation of fractional conversion ($CaCO_3$:$CaSO_4$) as a function of time at different temperatures (746, 771, 796, 846, 871 and 891°C). As expected, at a fixed time, the fractional conversion increases with temperature. At temperatures above 846°C, sulfation is completed by 2000 s. The reaction rate was calculated at each conversion. Figure 2 shows the modification of reaction rate with conversion at the different temperatures. It is evident that the sulfation rate decreases with sulfation degree and increases with temperature.

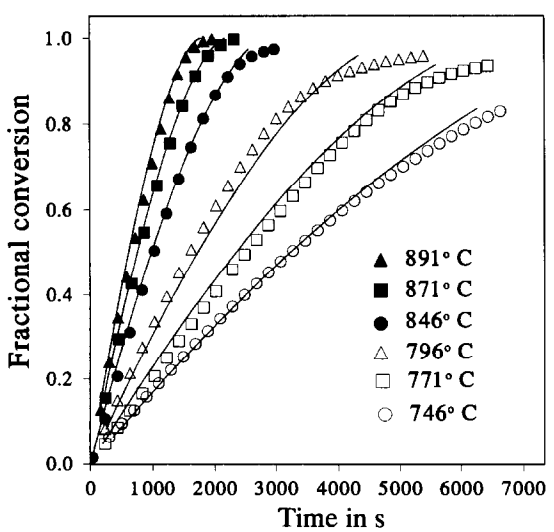

Fig. 1. Modification of fractional conversion with time at different reaction temperatures. Continuous line: model predictions.

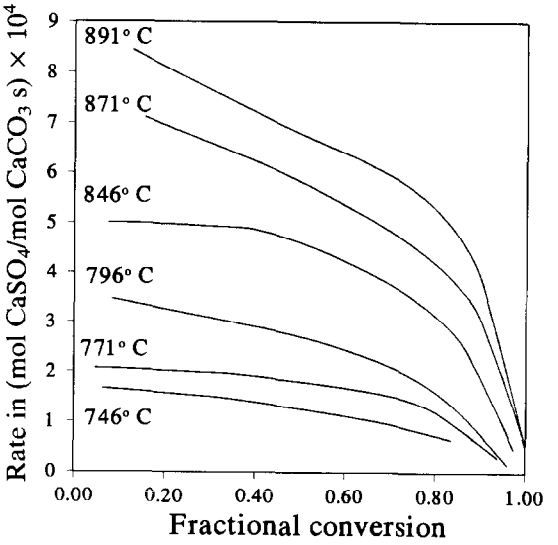

Fig. 2. Variation of reaction rate with sulfation degree at different reaction temperatures.

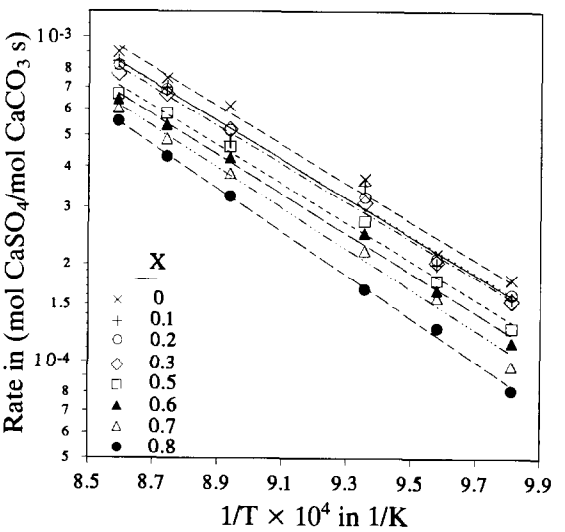

Fig. 3. Change of reaction rate with temperature at different sulfation degrees.

The influence of temperature on sulfation rate is illustrated in an Arrhenius plot (Fig. 3). The reaction rate at $X = 0$ was calculated by extrapolation at $t = 0$ of the experimental rate values. The activation energies corresponding to the slope of these least-squares lines are given in Table 1. At $X = 0$, the estimated value for the activation energy is 113 kJ mol^{-1}. At the beginning of the sulfation, before the formation of the product layer, the diffusional resistance is negligible and the

Table 1
Activation energy values at different sulfation degrees

Conversion	0	0.1	0.2	0.3	0.5	0.6	0.7	0.8
Activation energy/kJ mol^{-1}	113	113	112	112	114	117	120	128

process is considered to be chemically controlled. Then, the estimated activation energy at $X = 0$ (113 kJ mol^{-1}) corresponds to the chemical reaction.

The modification of the activation energy with conversion allows the changes in the rate-limiting processes to be examined. From the values indicated in Table 1, the activation energy hardly changes with conversion. This suggests that there is no change in the reaction regime with conversion and, in consequence, it can be concluded that the sulfation reaction takes place under chemical control up to high conversion degrees.

The direct sulfation of calcium carbonate particles proceeds according to a shrinking unreacted core model, as Hajaligol et al. [2] have already demonstrated. The overall process is a combination of chemical reaction at the interface and diffusion of gaseous reactants and products through the product layer. The overall reaction may be controlled by the chemical reaction or by the diffusion through the product layer.

As stated above, there are no arguments to support any type of diffusional control. There are two different explanations for the high mass transport coeffcients through the product layer: (a) the product layer exhibits a high porosity; or (b) mass transport takes place through a non-porous product layer, around the unreacted $CaCO_3$ grains, according to a solid–ionic mechanism and, under these circumstances, the diffusional rate is higher than the chemical reaction rate. The latter argument is more convincing because it is consistent with the high activation energies observed at high conversion degrees by some authors [6, 8, 9]. Moreover, it explains the differences found for the direct sulfation rates of calcium carbonate sorbents with different characteristics (raw limestones and pure $CaCO_3$ samples). In this sense, the solid–ionic diffusional rate increases with the concentration of lattice defects (structural defects or impurities). Thus, depending on the preparation method ($CaCO_3$) or impurities concentration (raw limestone), significant differences in the sulfation rate can be expected.

3.2. Modeling of sulfation reaction

In the modeling of the reaction between calcium carbonate particles and SO_2, it is assumed that the reactive surface at $t = 0$ is equal to the measured BET surface. This is equivalent to assuming that the calcium carbonate particles are formed by non-porous grains with a size of around 4 μm. These grains will react according to a shrinking unreacted core model. In consequence, they keep their original geometric shape during reaction. Then, by assuming a first-order reaction for SO_2, the relationship between the time and fractional conversion is given by [12]

$$t = \frac{1}{K_c} g_{F_g}(X) \tag{1}$$

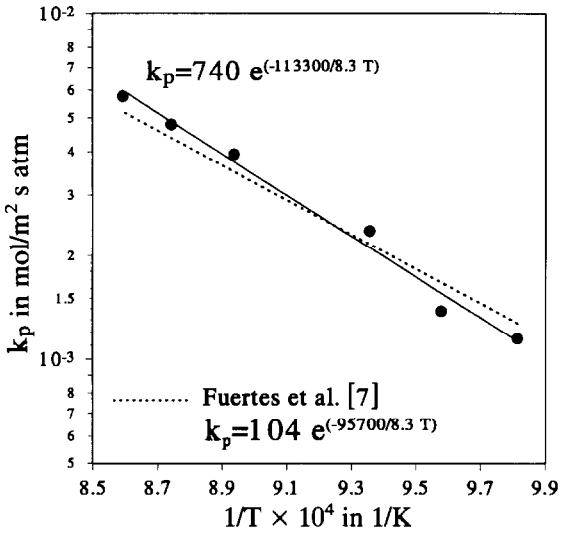

Fig. 4. Arrhenius plot of intrinsic rate constant.

where $K_c = k_p p S_0 / F_g$ and $g_{F_g} = 1 - (1 - X)^{1/F_g}$; k_p is the chemical rate constant, p the SO_2 partial pressure, S_0 the specific surface area at $t = 0$, and F_g the grain shape factor. Deriving Eq. (1)

$$\frac{dX}{dt} = k_p p S_0 (1 - X)^{1 - 1/F_g} \tag{2}$$

at $t = 0$

$$\left(\frac{dX}{dt}\right)_0 = k_p p S_0 \tag{3}$$

The intrinsic rate constant k_p can be calculated from the initial rate using Eq. (3). In Fig. 4 the variation of the estimated rate constants with temperature is represented in an Arrhenius plot. Kinetic parameters of $k_p = 740 \exp(-113300/RT)$ were derived from data fitting. In the same figure the values estimated by Fuertes et al. [7] from a raw limestone ($d_p = 25\ \mu m$ and $S_g = 0.42\ m^2\ g^{-1}$) are represented. A good agreement between the two sets of values is found.

The shape of the particles/grains is an important parameter in modeling gas–solid reactions. This problem is commonly avoided by assuming a spherical particle/grain shape ($F_g = 3$). The direct measurement of F_g parameter for particles with similar characteristics to those used here is a difficult task. However, the grain shape parameter can be estimated indirectly from the variation of the reaction rate with conversion. Thus, from Eqs. (2) and (3)

$$\left(\frac{dX}{dt}\right) \Big/ \left(\frac{dX}{dt}\right)_0 = (1 - X)^{1 - 1/F_g} \tag{4}$$

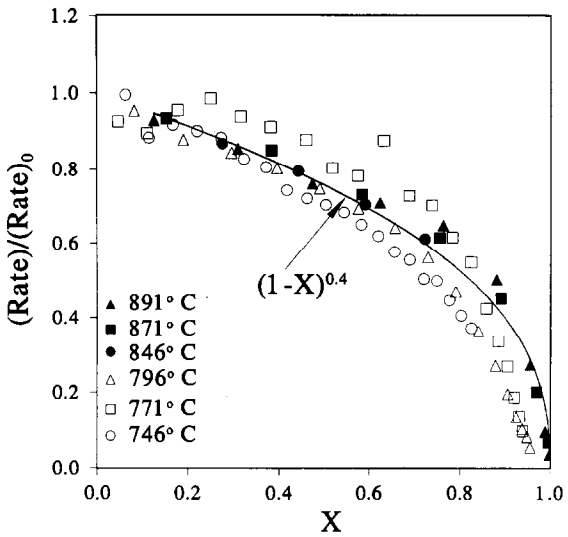

Fig. 5. Variation of (rate)(rate)$_0$ parameter with fractional conversion.

In Fig. 5 the variation of the $(dX/dt)/(dX/dt)_0$ ratio with fractional conversion X is represented for all temperatures. Using Eq. (4) for data fitting, a value of $F_g \approx 1.7$ $(1 - 1/F_g = 0.4)$ was found.

The introduction into Eq. (1) of the estimated k_p and F_g parameters allows the variation of fractional conversion with time to be predicted. In Fig. 1, the predicted $X-t$ curves are represented by a continuous line. A good agreement between the experimental data and those predicted by the model is found.

3.3. Comparision between sulfation of $CaCO_3$ and CaO sulfation

We were particularly interested in comparing the sulfation of $CaCO_3$ and CaO sulfation under similar conditions (temperature and SO_2 concentration). Some authors [2, 10] have reported higher conversion degrees for direct sulfation than for CaO sulfation. Figure 6 shows the variations of fractional conversion with time for the $CaCO_3$–SO_2 and CaO–SO_2 reactions at 891°C. For sulfation of calcined particles, two different regions can be detected. Up to $X \approx 0.7$, the variation of conversion with time for the CaO–SO_2 reaction is very similar to that for direct sulfation. Thereafter, the reactivity of the CaO–SO_2 reaction shows a sharp decrease. In consequence, whereas for direct sulfation the reaction was complete by 2000 s, the sulfation of calcined particles required times longer than 4000 s.

In Fig. 7 the variation of reaction rate ratio (rate of CaO–SO_2/rate of $CaCO_3$–SO_2) with conversion is represented. For low sulfation degrees, the calcined particles exhibit higher reaction rates than the $CaCO_3$ particles. This is so because the porous CaO particles have a higher reactive surface area than the calcium carbonate particles. As product layer formation in calcined particles occurs and pore plugging takes place, the reaction rate ratio decreases. For these particles, at

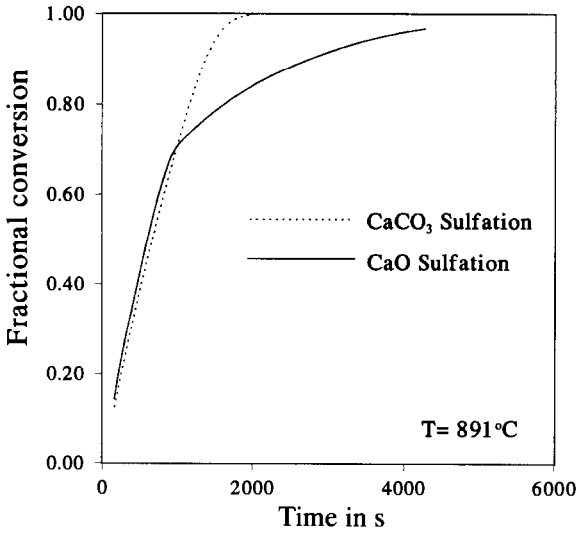

Fig. 6. Change of fractional conversion with time for $CaCO_3$ and CaO sulfation at 891°C.

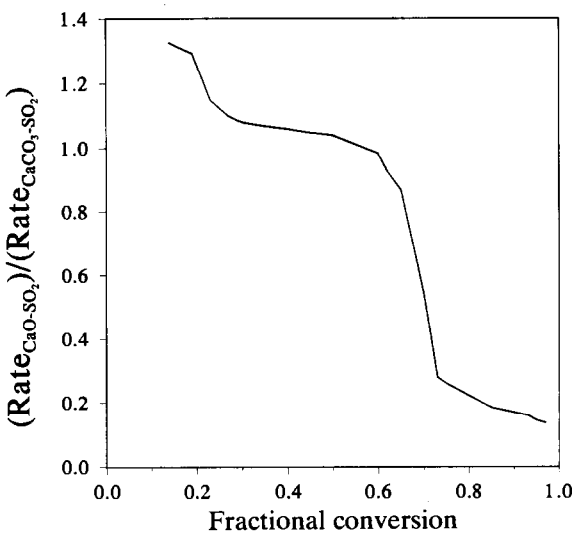

Fig. 7. Comparison of CaO sulfation rate with respect to $CaCO_3$ reaction rate ($T = 891$°C).

conversion degrees higher than 0.6 the reaction rate ratio decreases abruptly and the sulfation reaction of the CaO particles occurs slowly. This behavior can be explained by considering the observed differences in porosity of $CaSO_4$ formed during sulfation of $CaCO_3$ and CaO [2]. Thus, the high porosity of the external $CaSO_4$ formed during direct sulfation of $CaCO_3$ avoids plugging of the transport pores and allows gas diffusion through the particle. However, during sulfation of high porous CaO particles, a non-porous $CaCO_4$ layer is formed around the CaO

grains. At this stage the limiting resistances are solid–ionic diffusion through the product layer, for particle sizes of around 10 μm [13], or intra-particle gas diffusion, for particles bigger than 100 μm. As a consequence of the growing non-porous $CaSO_4$ layer, the blockage of transport pores occurs at a given sulfation degree. This provokes the collapse of the sulfation reaction because it thwarts gas diffusion to partially sulfated grains. In the described experiment (Figs. 6 and 7), sulfation collapse occurs at a sulfation degree of around 0.7.

3.4. *Sulfation of partially recarbonated calcined particles*

The gases in coal combustors (fluidized bed or pulverized boiler) are not perfectly mixed and consequently the gas composition changes from one part of the reactor to another. Thus, in high-pressure systems where the CO_2 partial pressure in the outlet gases is well above the equilibrium calcination pressure, there can be zones where the CO_2 partial pressure is below the equilibrium pressure and therefore calcination can take place. This situation is very probable in zones near the gas distributor. When the calcined particles are transported to a region of high CO_2 partial pressures, they react very quickly with CO_2 (recarbonation reaction).Tullin and Ljungström [14] observed that during this stage the recarbonation reaction dominates over the sulfation reaction. Then, it can be imagined that the sulfation reaction takes place between SO_2 and recarbonated particles instead of uncalcined calcium carbonate particles.

In order to study the differences between sulfation of uncalcined calcium carbonate particles and sulfation of recarbonated particles, a sample of $CaCO_3$ was calcined (in air), recarbonated in CO_2 at 850°C, and then sulfated at the same temperature (SO_2, O_2 and CO_2). Finally, the $CaSO_4$ formed was decomposed in air by heating to 1250°C. The complete experiment is shown in Fig. 8. Figure 9 illustrates the modification of fractional conversion with time: a. direct sulfation of uncalcined $CaCO_3$ particles; b. recarbonation of $CaCO_3$ calcined particles; c. direct sulfation of partially recarbonated particles. The results indicate that:

(i) During initial stages, the recarbonation reaction is very fast compared to sulfation reactions. After $X \approx 0.6$, the recarbonation rate diminishes abruptly. As a result, the reaction is not complete and only around 80% of the particle is recarbonated after 2000 s. This behavior is similar to that presented by CaO particles during sulfation and it can be explained as resulting from the blockage of transport pores [15]. Thus, it becomes evident that the recarbonated particles will be formed by $CaCO_3$ and CaO nuclei distributed throughout the particle.

(ii) During direct sulfation of recarbonated particles, two reactions occur simultaneously: sulfation of $CaCO_3$ formed during recarbonation, and recarbonation of residual CaO. A mean recarbonation rate of around 9×10^{-5} mol $CaCO_3$ per mol Ca s was estimated from the $X-t$ slope of the recarbonation reaction at times between 1500 and 2000 s. Using this value, the variation of sulfation degree with time during sulfation of recarbonated sample was estimated (Fig. 9). Although the recarbonation rate can be modified due to formation of a porous $CaSO_4$ layer, which enhances the CO_2 diffusion, it can be imaged that it only slightly affects the sulfation rate.

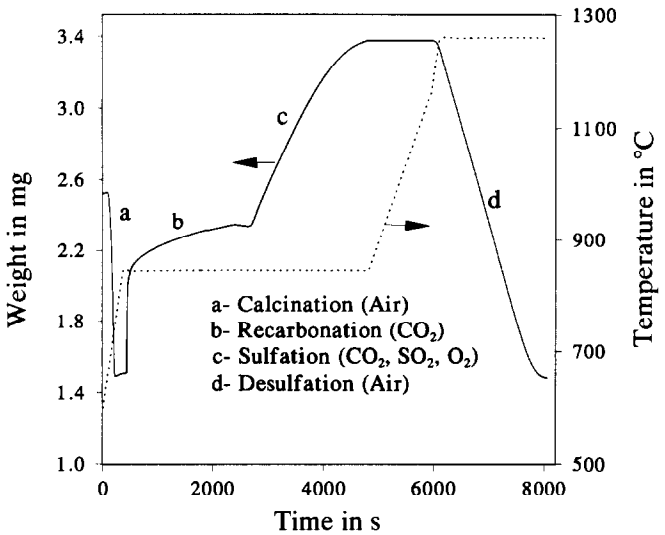

Fig. 8. TGA curve obtained during an experiment where the $CaCO_3$ sample was a, calcined; b, recarbonated; c, sulfated; d, the $CaSO_4$ formed decomposed.

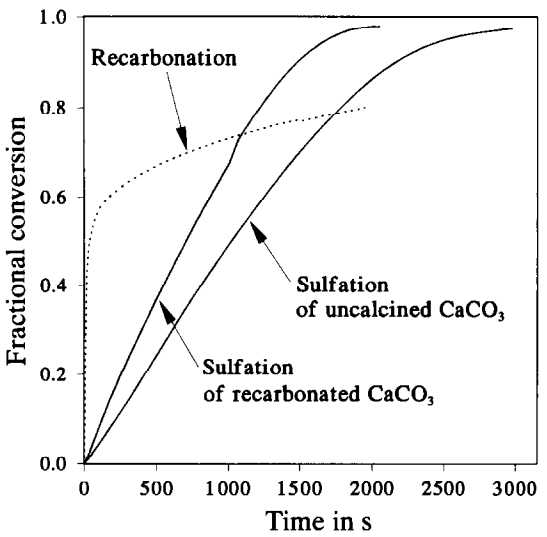

Fig. 9. Variation of fractional conversion with time during recarbonation of CaO, sulfation of recarbonated sample, and sulfation of uncalcined sample ($T = 850°C$).

The recarbonated sample exhibits higher sulfation rates than the uncalcined $CaCO_3$ sample (Fig. 10). The values found at 850°C for the sulfation rate at $t = 0$ were around 8.5×10^{-5} mol $CaSO_4$ per mol Ca s for the recarbonated samples and 5×10^{-5} mol $CaSO_4$ per mol Ca s for uncalcined sample. This difference can be explained by considering that the $CaCO_3$ layer of recarbonated sample exhibits a

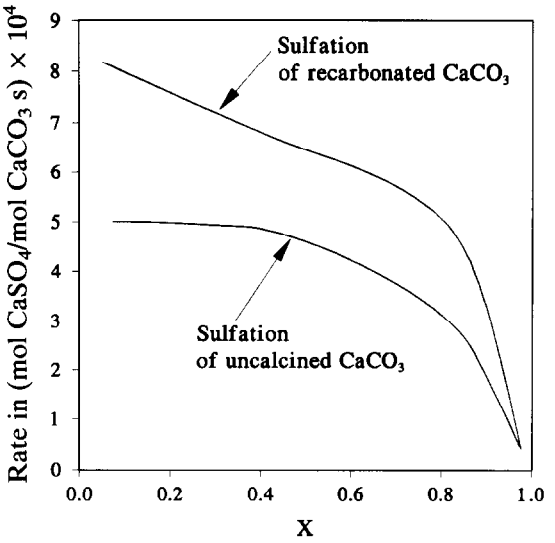

Fig. 10. Comparison of sulfation rates of recarbonated $CaCO_3$ and uncalcined $CaCO_3$ samples ($T = 850°C$).

higher reactive surface area than the uncalcined sample. This may be due to the nature of the $CaCO_3$ forming the two samples. In this respect, Tullin and Ljungström [14] have suggested that $CaCO_3$ crystallites are smaller in a recarbonated sample than in an uncalcined one.

4. Conclusions

From the variation of reaction rate with temperature at different sulfation degrees, it was deduced that the direct sulfation reaction is chemically controlled. An activation energy of around 110–130 kJ mol^{-1} was measured.

The process was modelled according to a shrinking unreacted core model. The particles are assumed to be formed by grains with an equivalent diameter of around 4 μm. The variation of sulfation degree with time is reasonably predicted using the deduced parameters, intrinsic rate constant, $k_p = 740 \exp(-113300/RT)$, and grain shape factor, $F_g = 1.7$.

From a comparison between CaO sulfation and direct $CaCO_3$ sulfation, it was deduced that, at low sulfation degrees, the calcined particles exhibit higher reaction rates than $CaCO_3$ particles. However, whereas the CaO sulfation reaction concludes abruptly at a given conversion, the $CaCO_3$ sulfation continues until complete conversion. In the former case, the end of sulfation is a consequence of the blockage of external pores. In the case of $CaCO_3$ sulfation, the formation of a porous $CaSO_4$ layer allows SO_2 to diffuse inside the particle.

The $CaCO_3$ particles formed from recarbonation of calcined particles exhibit higher sulfation rates than uncalcined $CaCO_3$ particles. This means that the sulfation reaction in a pressurized system probably occurs faster than expected from experiments performed with uncalcined $CaCO_3$ particles in a static reactor, i.e. a thermogravimetric analyzer.

Acknowledgment

The financial assistance of the DGCICYT (PB91-0101) is gratefully acknowledged.

References

[1] M.J.H. Snow, J.P. Longwell and A. Sarofim, Ind. Eng. Chem. Res., 27 (1988) 268.
[2] M.R. Hajaligol, J.P. Longwell and A. Sarofim, Ind. Eng. Chem. Res., 27 (1988) 2203.
[3] K. Iisa and M. Hups, 23th Symposium (Int.) on Combustion, The Combustion Institute, 1990, p. 943.
[4] K. Iisa, C. Tullin and M. Hupa, in E.J. Anthony (Ed.), 1991 Conference on Fluidized Bed Combustion, Montreal, ASME, New York, 1991, p. 83.
[5] J.B. Illerup, K. Dam-Johansen and K. Lunden, Chem. Eng. Sci., 48 (1993) 2151.
[6] C. Tullin, G. Nyman and S. Ghardashkhani, Energy and Fuels, 7 (1993) 512.
[7] A.B. Fuertes, G. Velasco, E. Fuente, J.B. Parra and T. Alvarez, in F. Kapteijn, J.A. Moulijn, K.A. Nater and W. Prins (Eds.), 3rd International Symposium on Coal Science, Rolduc, May 1993, Elsevier, Amsterdam, 1993, p. 65.
[8] A.B. Fuertes, G. Velasco, E. Fuente and T. Alvarez, Fuel Proc. Technol., in press.
[9] K. Iisa and M. Hupa, J. Inst. Energy, 65 (1992) 201.
[10] K. Iisa and M. Hupa, Conf. on Fluidized Bed Combustion, London, December 1991, Adam Hilger, Bristol, p. 191.
[11] R.H. Borgwardt, K.R. Bruce and J. Blake, Ind. Eng. Chem. Res., 26 (1987) 1993.
[12] J. Szekely, J. W. Evans and H.Y. Sohn, Gas–Solid Reactions, Academic Press, New York, 1976, Chap. 4.
[13] R.H. Borgwardt and K.R. Bruce, AIChE J., 32 (1986) 239.
[14] C. Tullin and E. Ljunhgström, Energy and Fuels, 3 (1989) 284.
[15] S.K. Bathia and D.D. Perlmutter, AIChE J., 29 (1983) 79.